Published in "Journal of African Earth Sciences 100: 586–597, 2014"
which should be cited to refer to this work.

Paleocene–Eocene palaeoenvironmental conditions of the main phosphorite deposits (Chouabine Formation) in the Gafsa Basin, Tunisia

László Kocsis [a,f,*], Anouar Ounis [b], Claudia Baumgartner [a], Claudius Pirkenseer [c], Ian C. Harding [d], Thierry Adatte [a], Fredj Chaabani [b], Salah Mohamed Neili [e]

[a] Institute of Earth Sciences, University of Lausanne, Switzerland
[b] Faculté des Sciences de Tunis, Université de Tunis El Manar, Tunisia
[c] Department of Earth Sciences, University of Fribourg, Switzerland
[d] Ocean & Earth Science, University of Southampton, National Oceanography Centre, UK
[e] Compagnie des Phosphates de Gafsa, Direction de Géologie, Métlaoui, Tunisia
[f] Geoscience Department, Universiti of Brunei Darussalam - UBD, Brunei Darussalam

A detailed sedimentary section of the marine Chouabine Formation in the palaeogeographic Gafsa Basin, south-western Tunisia, was investigated in order to characterize environmental and depositional conditions focusing on the interval that spans the Paleocene–Eocene transition. We did stable isotope analyses of bulk sediments. Both phosphorite and carbonate yielded relatively similar isotopic compositions; while marls show observable trends, with negative shifts in both $\delta^{13}C_{inorg}$ and $\delta^{18}O$ values at the Paleocene–Eocene transition.

The diversity of the calcareous microfossils is low. The presence of few environmentally tolerant small benthic foraminifera and the absence of planktic forms indicate a restricted palaeoenvironment subject to variation in salinity and temperature. The ostracod fauna is more diverse and is rather comparable to Paleocene and PETM (Paleocene–Eocene thermal maximum) assemblages in northwest Tunisia. While all these microfossils demonstrate various diagenetic features (i.e., phosphatization, secondary mineral overgrowths and infills), the different groups retain distinct stable isotopic compositions, suggesting partial preservation of signatures derived from their respective ecological niches.

Few organic-rich layers below the negative $\delta^{13}C$ shift yielded dinoflagellate assemblages with the common forms of *Adnatosphaeridium* sp., *Operculodinium* sp., *Spiniferites* spp. and *Thalassiphora* sp. The rare presences of *Apectodinium*-complex agree with depositional age prior to the PETM.

The combined data emphasize that most of the Chouabine Formation in the Gafsa Basin was deposited during the late Paleocene. The most negative isotopic values from marls are believed to represent the onset of PETM or pre-PETM record, and the related perturbation of the carbon cycle in shallow water deposits in Tunisia.

1. Introduction

Phosphate-rich marine sediments are well known in Tunisia and studied from the 19th century (e.g., Thomas, 1885; Pervinquiére, 1903; Visse, 1952; Burollet, 1956; Sassi, 1974; Fournier, 1980; Belayouni, 1983; Chaabani, 1995; Bolle et al., 1999; Béji-Sassi, 1999; Ben Hassen et al., 2009, 2010; Galfati et al., 2010; Ounis, 2011). The thickest deposits (up to 100 m) occur in the Gafsa Basin, an epicontinental basin which was palaeogeographically located between the Djeffara and Kasserine palaeo-islands (Fig. 1). Economically, the most important beds belong to the Chouabine Formation, which is intensively exploited in the region by the *Compagnie des Phosphates de Gafsa* (CPG). Despite numerous investigations, accurate dating of these phosphorite beds is difficult. The lack of precise biostratigraphy (Fig. 2a) largely relates to the poor preservation state of the microfossils mainly due to phosphatogenesis (Chaabani, 1995; Bolle et al., 1999). Moreover, in such shallow marine, coastal settings gaps in the sedimentary record often occur, and bioturbation and possible intrabasinal re-deposition may have caused further uncertainties. Therefore, there are discrepancies concerning the age of the Chouabine Fm. and the stratigraphic

* Corresponding author. Address: Geoscience Department, Faculty of Science, Universiti of Brunei Darussalam- UBD, Brunei Darussalam.
E-mail addresses: laszlokocsis@hotmail.com, laszlo.kocsis@ubd.edu.bn (L. Kocsis).

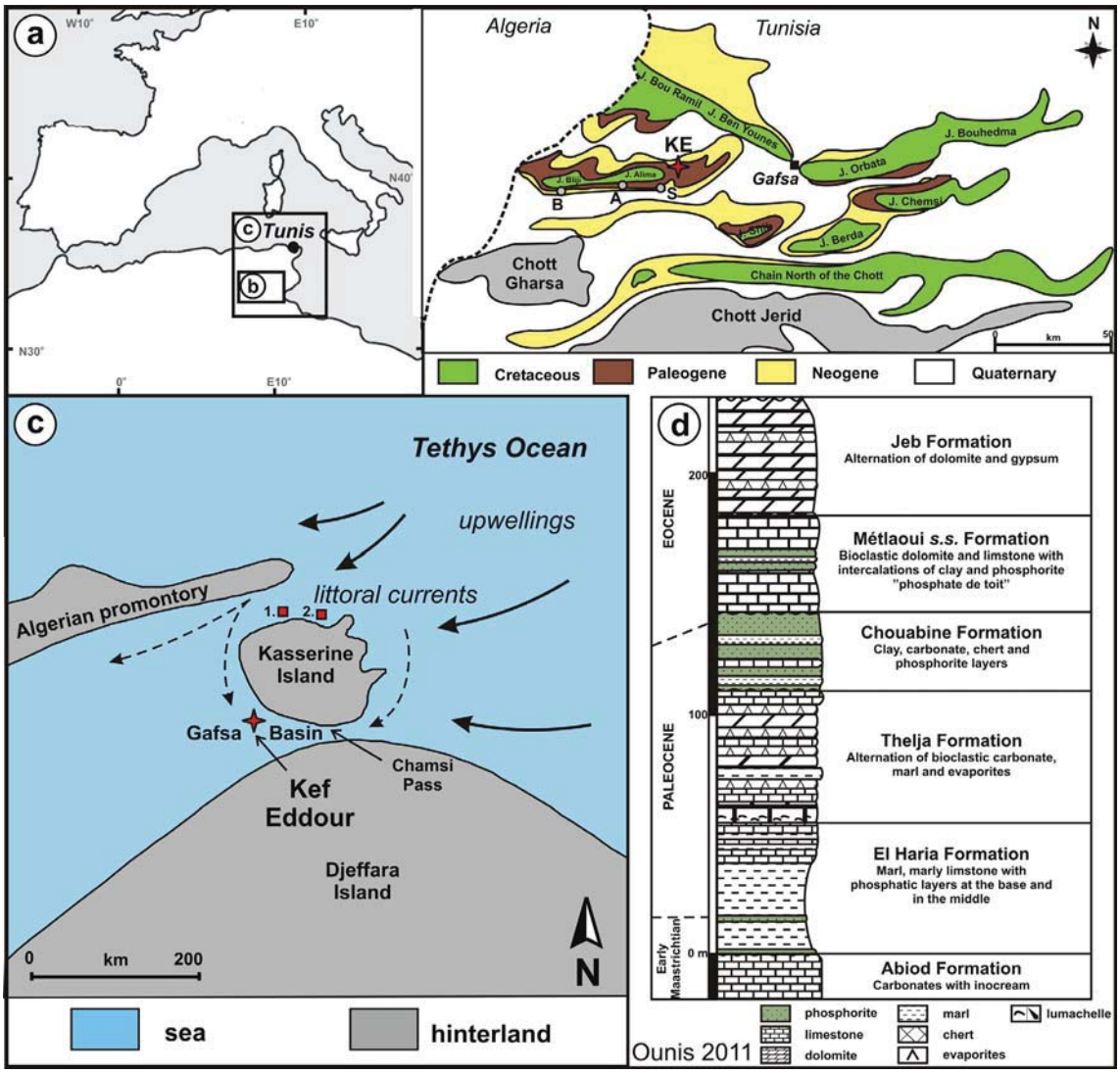

Fig. 1. (a) Location of the studied region. (b) Simplified geological map of the Gafsa Basin (extract from geological map of Tunisia 1/500,000). KE – the studied Kef Eddour section (red star). (A and B) Correspond to the Alima and Bilji sections respectively that were investigated by Ounis et al. (2008) (also see Fig. 2b), while S is for the Seldja section studied by Ben Abdessalam (1978) and Bolle et al. (1999). (c) Palaeogeographic situation in Tunisia during the late Cretaceous–early Paleogene (Sassi, 1974; Burollet and Oudin, 1980; Chaabani, 1995; Zaïer et al., 1998). The star marks the studied Kef Eddour section, while the numbers at the more open environment stands for (1) Sidi Nasseur and Wadi Mezaz (Morsi et al., 2011; Stassen et al., 2013) and (2) Elles (Bolle et al., 1999; Crouch et al., 2003). (d) General stratigraphy of marine deposits in the Gafsa Basin (Chaabani, 1995; Ounis, 2011). Note the major phosphorite-bearing levels marked by green. (For interpretation of the references to colour in this figure legend, the reader is referred to the web version of this article.)

position of the Paleocene–Eocene (P/E) boundary (Sassi, 1974; Ben Abdessalam, 1978; Fournier, 1980; Chaabani and Ben Abdelkader, 1992; Chaabani, 1995; Bolle et al., 1999; Ounis et al., 2008). More recent studies however corroborate that the Chouabine Fm. in the Gafsa Basin is largely of Paleocene age with only the top of the series attributed to the early Eocene (Ounis et al., 2008; Kocsis et al., 2013).

Phosphate-rich sediments crop out also north of the Kasserine palaeo-Island and they are also referred to as the Chouabine Fm. Here, the phosphorite beds deposited also during the late Paleocene/early Eocene (Zaïer et al., 1998). However phosphate formation occurred in smaller basins (e.g., Sra Ouertane) than the Gafsa and conditions were tended to be more oxic–suboxic due to better connection with the Tethys (Garnit et al., 2012). Other north-western deposits show major unconformities and the phosphorite rich levels seem to be restricted to the early Eocene (Morsi et al., 2011; Stassen et al., 2012).

During the Paleocene and Eocene several hyperthermal events have been recognized, and are coupled with negative carbon isotope excursions (CIEs; e.g., Zachos et al., 2001; Lourens et al., 2005). The warming and the isotopic shifts are interpreted as the consequence of geologically rapid injections of large volumes of ^{12}C-enriched carbon into the ocean/atmosphere system. These events were, thus geologically synchronous and, when coupled with age-diagnostic data, permit the recognition of individual climatic events that can be used to correlate Paleogene sedimentary sequences. In terms of magnitude, the largest (and most studied) CIE is the Paleocene–Eocene thermal maximum (PETM), an event which defines the P/E boundary (~55.8 million years ago-Ma) with a negative $\delta^{13}C$ shift of 2.5–6‰ (Kennett and Stott, 1991; Koch et al., 1992; Zachos et al., 2001; Thomas et al., 2002; Pagani et al., 2006).

Reasonably continuous sedimentary records in deep water sequences allow for a relatively easy correlation of these CIE events. However, in shallow marine environments, especially semi-confined basins such as the Gafsa Basin, enhanced local effects make stratigraphic correlation with reference deepwater

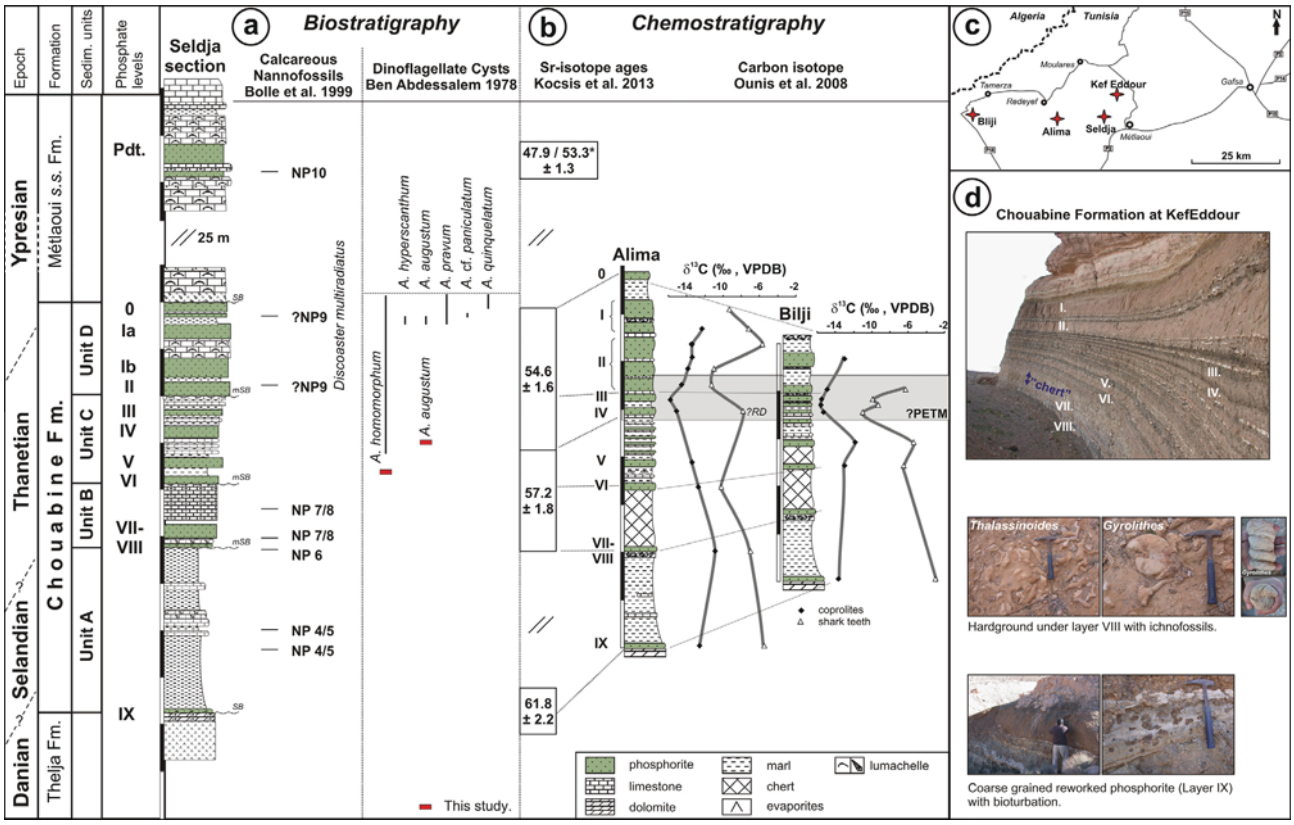

Fig. 2. Compilation of biostratigraphic (a) and chemostratigraphic (b) data in the Gafsa Basin from different sections (c). Note the main sedimentary units and the major phosphorite levels. Sr-isotope ages correspond to million years (My). In the Météaoui *s.s.* Fm. the Pdt. stands for "phosphate de toit". The Sr-age of these beds can yield two different ages (*) see Kocsis et al. (2013, Table 2). Abbreviations on plot (b) are PETM – Paleocene–Eocene thermal maximum, RD – possibly re-deposited sample. (d) The studied outcrop of the Chouabine Fm. with its characteristic sedimentary features. Note the different types of bioturbation.

successions more difficult. Nonetheless, the perturbations in the global carbon cycle influenced the atmosphere, hydrosphere, and biosphere, meaning that the carbon isotope shift was recorded in different archives in different environments (e.g., Koch et al., 1992; Aubry et al., 1996; Stassen et al., 2012; Yans et al., 2014; Kocsis et al., 2014). Hence, stable isotopic investigation of bulk sediment, and of organic matter or fossils could possibly reveal relative isotope shifts and may help improving local stratigraphy. In this context of the present study, Ounis et al. (2008) reported an up to 4‰ negative $\delta^{13}C$ shift from coprolites and shark teeth at phosphorite layers III–IV of the Chouabine Fm. in the Gafsa Basin (cf., Fig. 2 and in Ounis et al., 2008, Fig. 9). The large magnitude of this CIE and support from micropalaeontological data (Ben Abdessalam, 1978) lead the authors to correlate this shift with the PETM event, thus with the P/E boundary.

In order to further constrain the stratigraphy and palaeoenvironmental conditions in the Gafsa Basin, a new section in the Kef Eddour region were studied and sediments were collected between phosphorite layers I and VIII, focusing mainly on the interval that contains the reported negative CIE (Fig. 2b, Ounis et al., 2008).

2. Geological setting

During the late Cretaceous and early Paleogene a large part of Tunisia was covered by the southern Tethys, reflected by widespread shallow marine deposits (Fig. 1). The sediments indicate variable marine conditions from inner neritic to lagoonal environments relating to sea-level fluctuation and local tectonism (e.g., Sassi, 1974; Burollet and Oudin, 1980; Chaabani, 1995; Zaïer et al., 1998; Adatte et al., 2002). The Gafsa Basin was located between the Djeffara and Kasserine palaeo-islands (Fig. 1) and was connected to the open sea to the west. Restricted water exchange also occurred to the east through the Chamsi Pass (Fig. 1). The Upper Cretaceous–Lower Paleogene sedimentary sequence in the Gafsa Basin begins with the El Haria Formation, which overlies a hardground at the top of the chalky Upper Cretaceous Abiod Formation. Dark phosphate layer with glauconite and pyrite grains was initially deposited on the hardground, and passes upwards into a thick gray marl succession. This lithology is also common in north Tunisia, where it continued to accumulate during the Paleocene and early Eocene (Chaabani, 1995; Bolle et al., 1999; Zaïer et al., 1998). However, in the Gafsa Basin, new lithofacies were developed due to modification in marine conditions related to sea-level fluctuation and palaeogeographic reorganization. In the Paleocene, a bioclastic carbonate bed with intercalated lumachellic oyster, marly and gypsum-rich levels, was deposited named the Thelja ("Selja") Formation (Fournier, 1978; Chaabani, 1995). Above this formation, the Paleocene–Eocene Chouabine Fm. contains massive phosphorite layers which alternate with marly limestones, marls and silica-rich layers (e.g., Sassi, 1974; Chaabani, 1995). The thickness of the Chouabine Fm. can reach hundred meters with a certain variation through the basin (Chaabani, 1995). The formation represents a generally transgressive sequence, although smaller-scale sea-level fluctuations are apparent within the phosphorite succession and four sedimentary Units can be distinguished (A–D). Relative sea-level continued to rise during the deposition of the four Units and reached its maximum in the overlaying carbonate series of the Métlaoui Formation *Sensu Stricto* (Sassi, 1974; Chaabani and Ounis, 2008; Ounis, 2011). Later, the sea gradually retreated and the sedimentary sequence is topped by massive gypsum and dolomitic beds of the Jebs

Formation, which represents Sabkha depositional environments (Fig. 1, Chaabani, 1995; Zaïer et al., 1998; Ounis, 2011).

This study focuses on the phosphorite succession of the Chouanibe Fm. and the investigated part at Kef Eddour studied here is comparable with other sections at Selja locality (Fig. 2, Bolle et al., 1999; Adatte et al., 2002), at Alima Mountain (Ounis et al., 2008; Ounis, 2011), and at Oum El Khecheb region (Galfati et al., 2010), while at other sections this formation is more condensed (cf., Bliji Mountain – Ounis et al., 2008; Ounis, 2011; Ras-Draâ region – Ben Hassen et al., 2010).

The four sedimentary Units (A–D) of the Chouabine Fm. contain at least 10 major phosphorite layers (numbered from IX to 0; Fig. 2). The thickness of the units and the individual phosphorite layers is quite variable throughout the basin. In Unit A, the basal phosphorite bed, layer IX, is coarse-grained, bioturbated and contains many worn, re-worked shark teeth and coprolites (Fig. 2d). This basal phosphorite bed is overlain by marls and limestone. At the top of Unit A, the limestone level is topped by a strongly bioturbated hardground with frequent trace-fossils of *Thalassinoides* and *Gyrolithes* (Fig. 2d). Unit B starts with phosphorite layers VIII and VII. Up-section it consists of metre-scale silica-rich layer ("chert") that can be traced throughout the basin. The succeeding Unit C displays the greatest lithological variation: this unit begin with phosphorite layers VI and V, which are locally separated by marl. Further up-section various thin-bedded marl, limestone and phosphorite beds alternate. The Unit C is topped by the main phosphorite layers IV and III. At the top, Unit D is the richest in phosphate and layers II and I are the thickest phosphorite levels in the basin (up to 4 m). It is between Units C and D where the negative carbon isotope excursion (CIE) was detected by Ounis et al. (2008) and linked to the PETM, and hence to the Paleocene–Eocene boundary.

Palaeontological study of dinoflagellates in the Gafsa Basin indicates wider occurrence of the genus *Apectodinium* at the top of the series below the phosphorite layer 0 (Fig. 2a, Ben Abdessalam, 1978), which may be linked to the P/E transition (i.e., *Apectodinium* acme). This partly corroborates with calcareous nannoplankton data (i.e., NP9 zone, Fig. 2), however the preservation of these fossils are very bad (Bolle et al., 1999). The negative CIE observed by Ounis et al. (2008) lies slightly below this biostratigraphic range (Fig. 2b). On the other hand, Bolle et al. (1999) proposed the P/E transition at the top of the Chouabine Formation, mainly based on sequence stratigraphy and in comparison with the Elles section located north of the Kasserine Island (Fig. 1). Sassi (1974) also placed the P/E boundary between the Chouabine and Métlaoui *s.s.* formations. Other authors attribute the Chouabine Fm. entirely to the early Eocene (Fournier, 1980; Zaïer et al., 1998). Recently, Sr-isotope stratigraphy was attempted on the major phosphorite beds in the Gafsa Basin using well-preserved shark teeth (Fig. 2b, Kocsis et al., 2013). The ages obtained concur with the general stratigraphy of the basin and the proposed age-model matches the range of the P/E transitional beds (e.g., Ben Abdessalam, 1978; Ounis et al., 2008).

There is an obvious discrepancy considering the age of these beds that may be caused by a preservation bias of the microfossils. Incomplete preservation may be related to the phosphorite formation and/or may link to the environmental conditions of the semi-restricted basin. To further constrain the age and the depositional/palaeoenvironmental conditions of the phosphorite succession in the Gafsa Basin, stable isotope chemistry of bulk sediments were studied at Kef Eddour. In addition some layers were checked for microfossils content.

3. Methods

All the geochemical analyses were carried out in the laboratories of the Institute of Earth Sciences at University of Lausanne, Switzerland.

3.1. Whole rock samples

Between 100 and 200 g sediment from sixty-two levels were powdered and homogenized in an agate-mill. Four sub-sediment types were distinguished: phosphorite (32), carbonate (14), marl (15) and "chert" (1). These were analyzed for bulk stable oxygen and carbon isotopic compositions. The $\delta^{18}O$ and $\delta^{13}C$ values were measured using a Gasbench II coupled to a Finnigan MAT Delta Plus XL mass spectrometer (Spoetl and Vennemann, 2003). The analytical precision for this method was better than ±0.1‰. Oxygen and carbon isotopic compositions are expressed in the δ-notation relative to VPDB.

3.1.1. Total Organic Carbon (TOC) isotopic composition

Between 2 and 5 g sediment powder was pre-treated with 10% HCl for 24 h, then was washed several times and dried. The bulk residues were analyzed for $\delta^{13}C_{org}$ composition by flash combustion on an elemental analyzer (Carlo Erba 1108 EA) connected to a Thermo Fisher Delta V IRMS (EA/IRMS). The $\delta^{13}C$ values are reported relative to VPDB. The reproducibility of the EA/IRMS measurements for carbon is better than ±0.1. The accuracy of analyses was assessed using international reference standards.

3.1.2. Rock-Eval analyses

Sub-samples of the original sediment powders were subjected to Rock-Eval pyrolysis to analyse total organic and mineral carbon contents (TOC & MINC). The data were obtained using standard temperature cycle and expressed in weight percent (wt.%). The samples were bracketed by IFP 160000 standard from IFP, France, which had an error lower than 0.1% (Fig. 3).

3.2. Microfossils

Marly horizons intercalated in the phosphorite succession were disaggregated with 10% H_2O_2, then washed with distilled water and wet-sieved (mesh size 100 and 300 μm) to extract calcareous microfossils. The fossils were picked under a binocular microscope and their preservation was examined using a laser confocal microscope (Olympus LEXT, OLS4100) both with laser and natural light, and a Tescan Mira LMU scanning electron microscope (SEM) at the University of Lausanne (Fig. 4, Plate 1). In some cases, energy-dispersive X-ray spectra (EDS) were recorded to test major element composition of the specimens and related secondary mineral infill or overgrowths (Fig. 4). The most well preserved fossils were measured for stable isotopic compositions following the same procedure as for the whole rock samples.

Four clay-rich layers were analyzed for dinoflagellate cysts in order to obtain further biostratigraphic and palaeoenvironmental data. Palynological processing techniques outlined in Wood et al. (1996) were used, including stepwise dissolution of the sediments in hydrochloric acid (32%) followed by HF (60%), boiling in HCl (10%), and brief oxidation in nitric acid (30%), before being mounted on glass slides for light microscopic examination. Sample preparation was carried out in the Palynology Lab of University of Southampton (UK). Transmitted light images were taken at University of Lausanne using a multi-image, extended focus technique on a VS-110 Virtual Slide System of Olympus (Plate 2). Dinoflagellate cyst nomenclature follows that of Fensome and Williams (2004).

4. Results

4.1. Bulk sediments

The Rock-Eval analyses confirmed field-observations of the mineral carbon content being higher in carbonate-rich levels

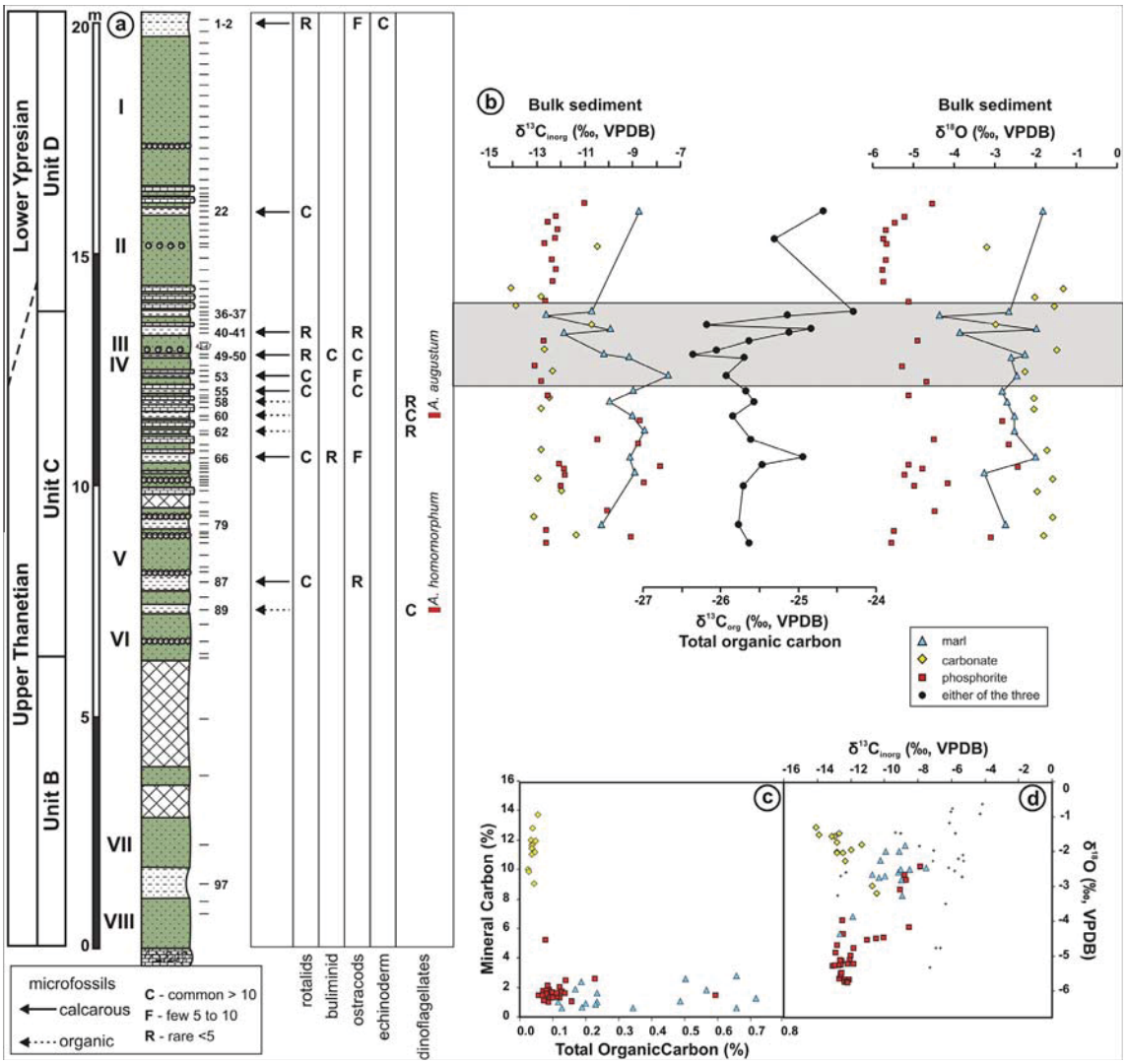

Fig. 3. (a) The Kef Eddour stratigraphic log showing the sampled horizons and the recovered fossils. (b) Stable isotope values for bulk sediments ($\delta^{13}C_{inorg}$ and $\delta^{18}O$) and total organic carbon ($\delta^{13}C_{org}$). The gray band marks the place of carbon isotope excursion reported by Ounis et al. (2008) (see Fig. 2b). (c) Total organic carbon versus mineral carbon concentrations obtained by Rock-Eval analyses. (d) $\delta^{13}C_{inorg}$ versus $\delta^{18}O$ of the bulk sediments. Black crosses are data from calcareous microfossils (cf. Fig. 5). Note the separations of the different sediment types on the plots in (c) and (d).

(11.4 ± 1.2 wt.%, $n = 13$) than in the phosphorites and marls (1.8 ± 0.8 wt.%, $n = 25$ and 1.4 ± 0.7 wt.%, $n = 16$, respectively; Fig. 3d). In terms of TOC, the samples generally show very low concentrations (<0.2 wt.%), with only few marl samples yielding TOC values higher than 0.5 wt.% (Fig. 3).

The stable isotopic compositions of the phosphorite beds show large variations ($\delta^{13}C = -11.7 \pm 1.5‰$ and $\delta^{18}O = -4.8 \pm 0.9‰$, $n = 32$). The $\delta^{13}C$ values are similar to those of the carbonates but much lower than measured in the marls (−9.7 ± 1.3‰, $n = 15$). In terms of the $\delta^{18}O$ isotopic compositions, both carbonates and marls yielded higher values of −2.0 ± 0.5‰ ($n = 14$) and −2.7 ± 0.7‰ ($n = 15$), respectively. The stable isotope values of the one silica-rich level are within the range of the marls. Carbonate content was calculated for each sample from the CO_2 yield of the stable isotope analyses comparing to the yield of pure calcite (i.e., Carrara marble standard). The results agree with the data obtained from the Rock-Eval analyses. The carbon isotopic composition of residual organic matter in the sediments ranges from −26.4‰ to −24.3‰ ($n = 22$). The calculated yields for TOC content are generally in accordance with the Rock-Eval analyses.

The complete dataset can be found in Tables 1–3 of the electronic supplementary material.

4.2. Microfossils

The phosphorite samples yielded many well-preserved bioapatite fossils, such as tiny shark and ray teeth, scales and spines, whereas calcareous fossils are rare and the only recovered are completely phosphatized molds.

Nine marl levels yielded identifiable calcareous microfossils (S1-2; S41, S49-50, S53, S55, S66 and S87, cf. Fig. 3). Only a few poorly preserved remains or molds were discovered in other samples. The calcareous fauna is of low diversity and consist of few small benthic foraminifera, ostracods and in the uppermost samples, echinoderm spines (Plate 1, Fig. 4). Planktic foraminifera are entirely absent. Various secondary mineral infill, such as calcite, silicates or secondary dolomite are apparent both in and on the fossils. In addition, phosphatization processes have also affected the calcareous tests and dissolution and partial phosphatization of the microfossils are commonly observed (Fig. 4).

The ostracod genera *Paracosta*, *Reymenticosta*, *Buntonia*/*Protobuntonia* and *Alocopocythere* were identified, though the poor preservation and scarce material only allowed tentative determinations. The diversity of the benthic foraminifera is very low and restricted to small rotalid and buliminid forms, with the dominance

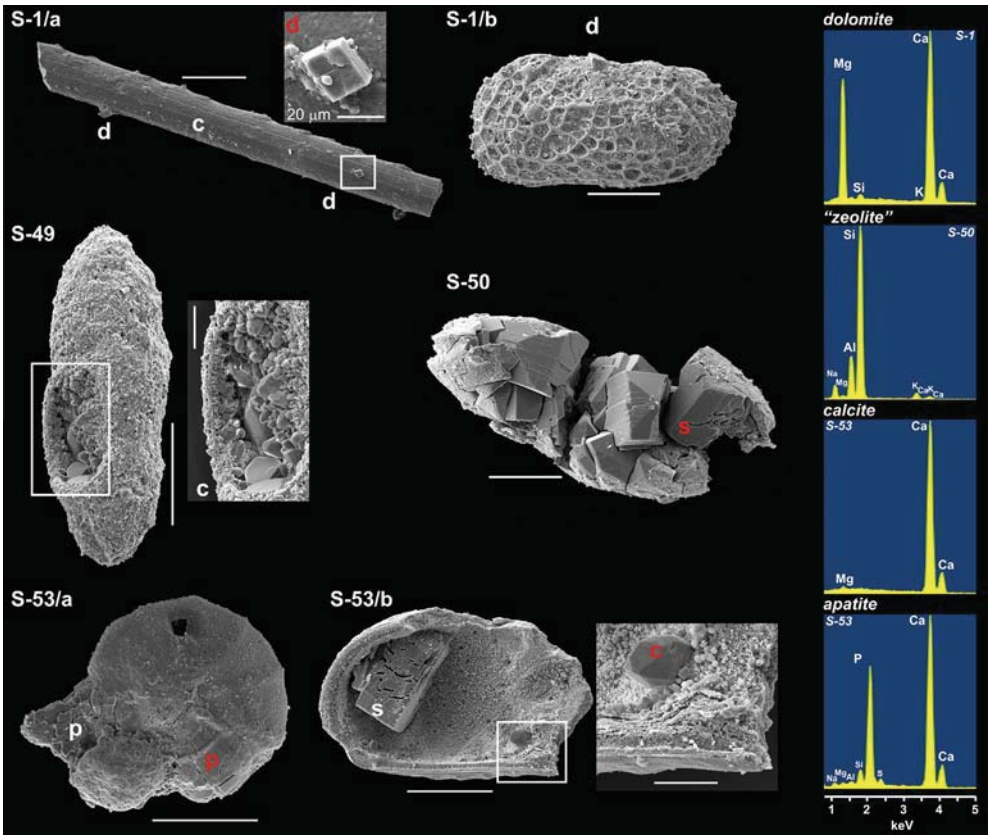

Fig. 4. Calcareous microfossils and related diagenetic features. Numbers indicate stratigraphic positions of the samples (see Fig. 3). S1/a – echinoderm spine; S1/b – ostracod; S49 – buliminid foraminifera; S50 – ostracod mold; S53/a – rotalid foraminifera; S53/b – ostracod valve. Scale bars: 200 µm, cut-outs 50 µm and 20 µm. Abbreviations: c – calcite, d – dolomite, s – silica-rich phase, most likely a zeolite, p – phosphate (apatite). The marked in red corresponds to EDS spectrum measurements. (For interpretation of the references to colour in this figure legend, the reader is referred to the web version of this article.)

changing between these groups in any given layer. Among the rotalid genera *Anomalinoides*, *Elphidiella* and a few *Cibicidoides* are present, while buliminids are represented by *Bulimina* spp. and *Stainforthia* spp. The latter genera are especially frequent in the marls between phosphorite layers III and IV.

Some better preserved specimens were analyzed for their stable isotopic compositions. Secondary calcite infill, however, could not be avoided entirely, which may have altered the original *in-vivo* isotopic signal. Still, clear separations among ostracods, buliminids and rotalids are apparent in the data (Fig. 5). Rotalids and buliminids yielded $\delta^{18}O$ values of $-2.3 \pm 0.2‰$ ($n = 7$) and $-2.9 \pm 0.4‰$ ($n = 3$), respectively. Ostracods generally show higher $\delta^{18}O$ values ($-1.2 \pm 0.4‰$, $n = 9$), with the exceptions of some specimens from the uppermost marl layers that yielded much lower $\delta^{18}O$ values ($-4.6 \pm 0.8‰$, $n = 4$). Buliminids show the lowest $\delta^{13}C$ values of $-12.6 \pm 0.3‰$ ($n = 3$), while ostracods ($-6.6 \pm 1.5‰$, $n = 13$) and rotalids ($-6.3 \pm 1.0‰$, $n = 7$) yielded similar, but more variable values. The stable isotopic compositions of echinoderm spines overlap with the isotopic values of the rotalids.

Two of four palynological samples investigated (S60 and S89) yielded dinoflagellate floras (Plate 2). The most abundant species by far is *Adnatosphaeridium multispinosum* in both samples. Additionally the *Operculodonium* spp. and *Spiniferites* spp. are quite frequent, while *Thalassiphora* is common only in sample S60. Typical late Paleocene–early Eocene forms of *Apectodinium* are rather rare. *Apectodinium homomorphum* is present in sample S89 and a single specimen of the PETM-diagnostic *Apectodinium augustum* was found in sample S60. Other taxa are infrequent and represent only a small part of the flora (Plate 2).

5. Discussion

5.1. Depositional palaeoenvironment

The main facies types of the Chouabine Fm. – phosphorite, marl, and carbonate – are well distinguished by their mineral and organic carbon contents and more importantly, by their stable isotopic compositions (Fig. 3). The absolute values of inorganic $\delta^{13}C$ for all lithologies are very low compared to open marine sediments or other phosphorite deposits (McArthur et al., 1980; Shemesh et al., 1988; Kolodny and Luz, 1992; Lerman and Clauer, 2007). This reflects an early shallow-burial environment, in which enhanced oxidation of organic matters lowered the isotopic composition of dissolved inorganic carbon (DIC) in the pore fluids (McArthur et al., 1986; Shemesh et al., 1988; Lawrence, 1989; Martin and Sayles, 2003). Therefore, any carbonate-bearing authigenic minerals precipitated in the sediments inherited this low $\delta^{13}C$ composition, and possibly low $\delta^{18}O$ too. The lowest $\delta^{13}C$ and $\delta^{18}O$ values come from the phosphorites, further emphasizing the intensive organic matter recycling, which provided phosphorous for the authigenic phosphate formation (Prévôt, 1990; Lucas and Prévôt-Lucas, 1996). The occasional marine connection to the Tethys in the east could have brought upwelling-derived nutrient-rich seawater into the Gafsa Basin, hence increasing bioproductivity and consequently organic influx to the seafloor (e.g., Chaabani, 1995). The $\delta^{13}C_{org}$ values of the TOC support a marine origin, although a continental influence cannot be ruled out entirely based only on the isotope data (Hoefs, 2004).

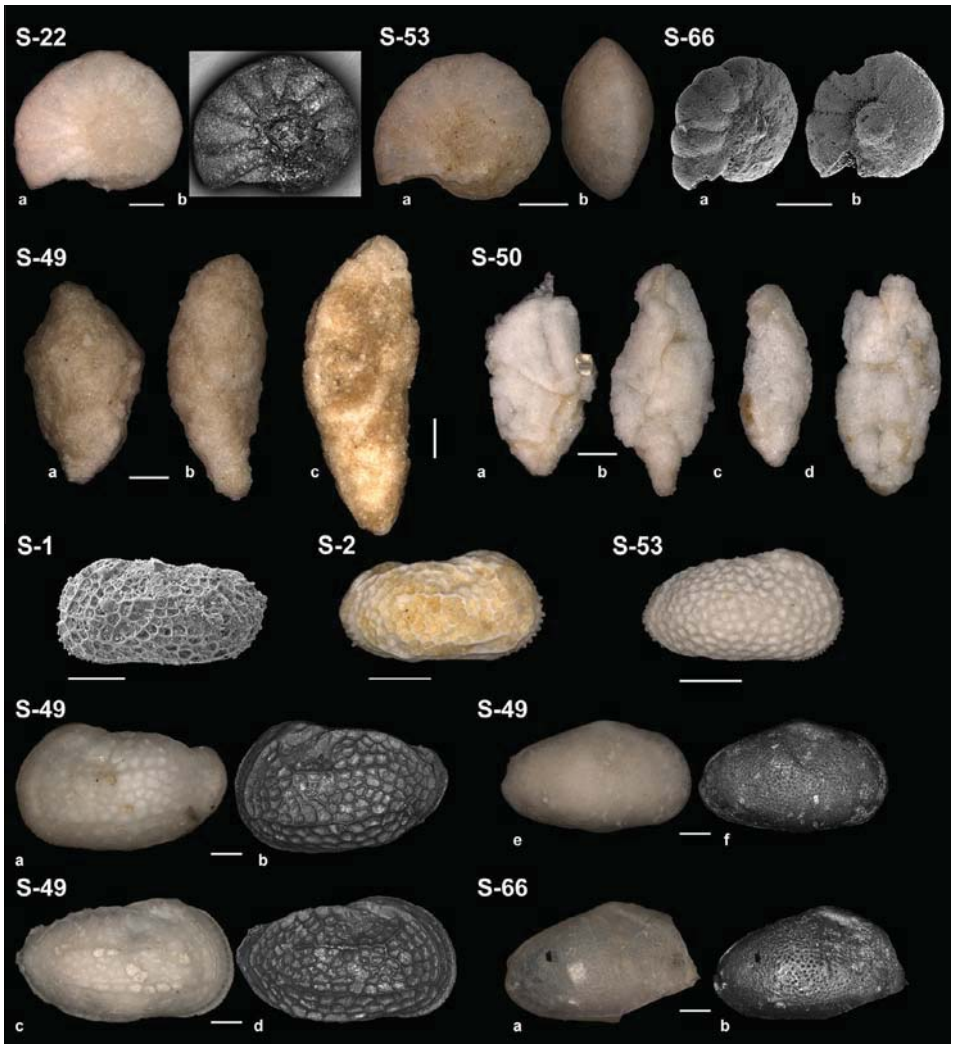

Plate 1. Calcareous microfossils. Numbers correspond to stratigraphic positions (see Fig. 3). Top row: rotalid foraminifera (S22 a–b [NL-LL], S66 a–b [LL] – *Elphidiella* spp., S53 [NL] – *Anomaloides* spp. (slightly oblique view). Second row: buliminids (S49 a–c [NL] – *Bulimina* spp. S50 a–d [NL] – *Stainforthia* spp.). Lower half of the plate, ostracods: S1 [SEM] – cf. *Paracosta parakefensis*; S2 [LL] – cf. *Paracosta parakefensis*; S49 a–b [NL-LL] – *Reymenticosta* sp.; S49 c–d [NL-LL] – *Reymenticosta* sp.; S49 e–f (NL-LL] – aff. *Buntonia? tunisiensis*; S53[LL] – cf. *Alocopocythere attitogonensis* juv.; S66 a–b [NL-LL] – cf. *Protobuntonia nakkadii*. Scale bars: 200 µm. [Images are taken by: NL – natural light; LL – laser light; SEM – Scanning electron microscope.]

However, the exceptionally low $\delta^{13}C_{inorg}$ values in the sediments could be indicative of early depositional conditions that may have approached diagenetic zones of denitrification or even sulfate reduction (McArthur et al., 1986; Piper and Kolodny, 1987). However, bottom water and probably also the upper part of the pore-fluid in the sediments must have been well-oxygenated, as indicated by frequent bioturbation (cf., Fig. 2). Moreover, the rare earth element distribution and Ce-anomaly of biogenic apatites are linked to oxic–suboxic burial conditions (Ounis et al., 2008). Therefore, sulfate reduction and anoxic conditions were not reached during early diagenesis.

This shallow water environment, associated with the semi-confined palaeogeographic situation of the Gafsa Basin (Fig. 1c), induced phosphorite formations. Phosphatization is also apparent on a microscale and in the other sediments as well. Calcareous microfossils recovered from the marls show partial phosphatization of their tests (Fig. 4). Such processes in the phosphorite layers are common (e.g., Lamboy, 1993), and completely phosphatized molds of calcareous remains are frequently found. There are other diagenetic features that can be linked to the phosphatization: (1) secondary dolomite growth is often observed on the calcareous fossils (Fig. 4) and (2) individual dolomite rhombohedra are frequent in the phosphorite layers. The precipitation of dolomite reduced the magnesium ion concentration in the pore fluid, which element is known as an inhibiting factor for phosphate precipitation (e.g., Nathan, 1984; Prévôt, 1990), therefore phosphogenesis could be enhanced.

Secondary calcite and silica-rich mineral infill are other diagenetic features on the calcareous fossils (Fig. 4). The silicate minerals are most likely a type of zeolite (i.e., clinoptilolite), already known from marine sequences in the region (Sassi and Jacob, 1972; Sassi, 1974; Galfati et al., 2010; Ounis, 2011), which originated from diagenetic dissolution of siliceous skeletons (e.g., siliceous sponges, diatoms). Unfortunately, the insufficient amount of these remains at Kef Eddour did not allow us to analyse the mineralogy by X-ray diffraction (XRD), but the EDS spectra confirm our hypothesis (Fig. 4). Interestingly, these "zeolites" form entire ostracod molds, often without any preservation of the calcareous test, even if other calcareous fossils are preserved and show secondary calcite growth in the same bed (cf., S49-50 at Fig. 3). These molds are thus perhaps reworked and derived from older beds, where the burial fluid had a lower pH and dissolved the carbonate valves.

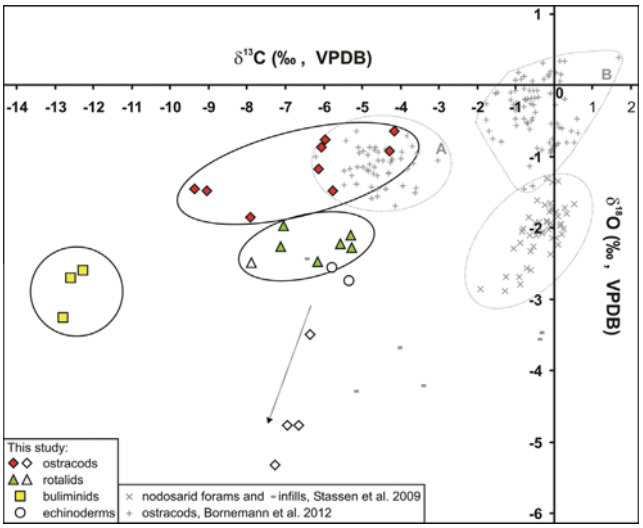

Fig. 5. Stable isotopic compositions of calcareous microfossils from Kef Eddour. For comparative purpose data from the Sidi Nasseur section (cf. Fig. 1) are plotted as well. Danian smooth (A) and ornamented (B) ostracods (Bornemann et al., 2012) and Thanetian nodosarid foraminifers (Stassen et al., 2009). Note the three major clusters at Kef Eddour corresponding to buliminids, rotalids and ostracods. Their oxygen isotopic compositions are very similar to the Sidi Nasseur data. Exceptions are some ostracods with lower $\delta^{18}O$ values from the uppermost samples of the succession (S1-2 – samples marked in white). From this level the echinoderms group with the rotalids. The arrow indicates possible diagenetic trend toward lower $\delta^{18}O$. Note that similar low values obtained from calcite infill of foraminifers at Sidi Nasseur.

5.2. Microfauna – preservation and biostratigraphy

The low diversity of foraminifera and the lack of planktic forms may suggest a preservation bias in view of the diagenetic features discussed in the previous paragraph. However, the restriction of the depositional environment during the Paleocene/Eocene boundary times almost certainly excluded the presence of planktic foraminifera due to highly variable salinity and temperature as well as a relatively shallow water depth in the Gafsa Basin. On the other hand, the small benthic genera *Anomalinoides*, *Elphidiella* and buliminids in general (Plate 1), are known for their tolerance to extreme conditions and could indicate even temporarily hyposaline conditions (Jorissen et al., 1995; Stassen et al., 2009, 2012). Other proxies however such as clay mineralogy of the sediments (Bolle et al., 1999), support rather evaporative, arid conditions (i.e., hypersaline), therefore the presence of these taxa may link to occasional, freshwater influx to the basin (i.e., brackish condition). The fauna also possibly includes some endemic forms, which for now, have a low significance for biochronology. Hence altogether, their presence can be linked to the stressed environment resulting from the semi-confined palaeogeographic condition of the basin. The ostracod faunas on the other hand closely resemble the Paleocene and PETM assemblages reported from northwest Tunisia (Morsi et al., 2011). Their preservation and low numbers, however, hinder a detailed statistical comparison.

Despite being altered by diagenesis, the different microfossils show discrete stable isotopic compositions (Fig. 5):

1. Buliminids show distinctly lower $\delta^{13}C$ values compared to the other fossils. This group of benthic foraminifera is known for its tolerance to oxygen-deficient environments (Van der Zwaan et al., 1999). Hence, their low $\delta^{13}C$ values may correlate with a deeper infaunal habitat (Kouwenhoven et al., 1997; Ernst et al., 2006; Stassen et al., 2012) characterized by pore waters depleted in oxygen and enriched in light DIC due to a high flux of organic matter.
2. However, rotalids, ostracods and echinoderms show less negative $\delta^{13}C$ values that may correlate with their epibenthic or shallow infaunal habitats characterized by waters richer in oxygen and heavier DIC. Interaction with porefluid during early diagenesis clearly altered the geochemistry of the fossils as the absolute $\delta^{13}C$ values are too low relative to normal marine conditions (Lerman and Clauer, 2007) and other Tunisian data from more open environment (Fig. 5). Nonetheless it seems the relative ecological offsets in the $\delta^{13}C$ values are preserved in the microfossils (Fig. 5).

Conversely, the $\delta^{18}O$ composition of the fossils is much closer to normal marine environment (>−3‰; e.g., Wefer and Berger, 1991). However the relatively low values may also reflect to some extent the early diagenetic environment. Nevertheless, the $\delta^{18}O$, and partially the $\delta^{13}C$ values of ostracods are in the range reported from Sidi Nasseur section located at north-western Tunisia (Fig. 5), a site that had good connection to the open ocean (Bornemann et al., 2012). Exceptions are those specimens from the topmost layer of the succession with $\delta^{18}O$ values as low as −5.5‰ that may indicate freshwater influence (cf., S1-2, Figs. 3 and 5).

A low diversity organic-walled dinoflagellate flora was recovered from some organic-rich layers at Kef Eddour (Plate 2). Ben Abdessalam (1978) studied dinoflagellate cysts in details from the phosphorite sequence at Seldja. The author placed the P/E boundary in the upper part of Unit D (cf., Fig. 2a) based on amplified abundance and diversity of the Wetzeliellaceae (i.e., *Apectodinium* complex). *Apectodinium* was present in the Southern Tethys already in latest Danian (Fig. 6a, Hardenbol et al., 1998) and became more common, at least from P4b foraminiferal subzone (cf., Crouch et al., 2003). In Unit C at Kef Eddour the *Apectodinium* complex is present (Plate 2) but rather scarce, which concurs with the Ben Abdessalam's work and would emphasize that the major part of Unit C is deposited in the Paleocene. The rare presence of *A. augustum* at Kef Eddour may further suggest a latest Paleocene age if the biostratigraphic significance of this species is followed (Williams et al., 2004; Sluijs et al., 2007; Gradstein et al., 2012). These interpretations are in agreement with other biostratigraphic data derived from calcareous nannofossils (Bolle et al., 1999; Fig. 2). Though these fossils are poorly preserved, it still allows the identification of NP7/8 and somewhat uncertain NP9 nannoplankton zones dated to late Paleocene and earliest Eocene.

5.3. Stable isotope chemostratigraphy

The stable carbon isotope data of bulk sediments from the Kef Eddour locality yielded stratigraphic variations that are largely influenced by the lithology. Phosphorites and carbonates show rather low and homogenous $\delta^{13}C_{inorg}$ values along the series. Exceptions are phosphorites that have higher carbonate content. However, the marl levels show generally higher carbon isotopic values, with a small negative trend from the phosphorite layer IV up to the border of Units C and D (Fig. 3). This is the same interval where Ounis et al. (2008) reported CIEs from other successions within the Gafsa Basin and linked it to the global PETM event (Fig. 2). Clearly local processes were important in the Gafsa Basin, but even if they overprint the global signal, such as observed in the phosphorites, the bulk $\delta^{13}C_{inorg}$ values of the marls may have retained the imprint of the PETM.

In the top of the negative $\delta^{13}C_{inorg}$ interval the marls also yielded negative $\delta^{18}O$ spikes (~2‰, Fig. 3b). These data fit the characteristics of the PETM, such as the sudden warming, which is represented by globally recognized negative $\delta^{18}O$ shifts in the marine record (Zachos et al., 2008). These negative values of the marls may represent this warming; however, shark teeth and

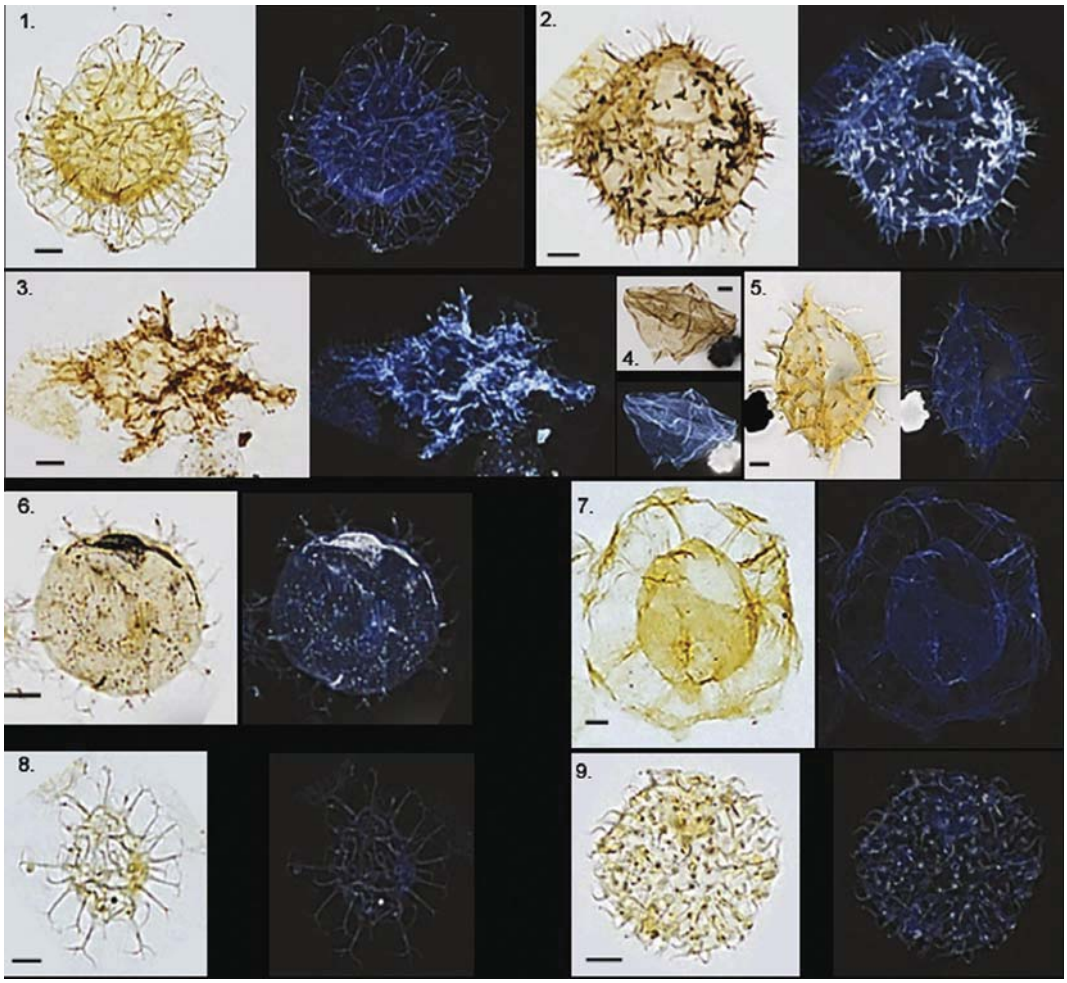

Plate 2. Dinoflagellates. Two images are provided for each specimen, one as a positive light microscope image and a second negative image to emphasize some of the features not seen in normal light. (1) *Adnatosphaeridium multispinosum* (S60); (2) *Apectodinium homomorphum* (S89); (3) *Apectodinium augustum* (S60); (4) ?*Phelodinium magnificum* (S89); (5) *Fibrocysta* cf. *bipolaris* (S89); (6) *Hafniasphaera* spp. (S89); (7) *Thalassiphora* cf. *patula* or *pelagica* (S60); (8) *Spinifer* spp. (cf. *ramosus*) (S89); (9) *Operculodinium* spp. (S89). Scale bars: 10 μm.

coprolites from the Gafsa Basin did not show negative changes in their oxygen isotopic compositions at the CIE (Ounis et al., 2008). This could be explained by local effects such as very warm and arid climatic conditions and enhanced evaporation existing in the semi-closed Gafsa Basin (Ounis et al., 2008; Kocsis et al., 2013). The localized processes are further highlighted by the rather uniform $\delta^{18}O$ values of the bulk phosphorite across the P/E boundary. The oxygen isotopic composition of structural carbonate in phosphate is more prone to diagenetic alteration (e.g., Zazzo et al., 2004) and the overall, rather constant and low $\delta^{18}O$ values in these sediments would reflect homogenization process in relation to phosphatization.

The $\delta^{13}C_{org}$ compositions of the sediments show minor fluctuations between −24‰ and −26.5‰ through the succession studied but no distinct CIE is apparent (Fig. 3). This is somewhat surprising if the CIE in the inorganic phase is linked to the PETM. The $\delta^{13}C_{org}$ data from the combined sections of Sidi Nasseur and Wadi Mezaz north of the Kasserine Island (Fig. 1c) clearly reflects the main characteristics of the PETM event (Fig. 6, Stassen et al., 2013), however the carbonate $\delta^{13}C$ does not show CIE there (Stassen et al., 2013). Observing the opposite trend in the Gafsa Basin could be explained by local processes, most possibly by the intensive organic matter recycling (i.e., low TOC content, Fig. 3c) that links to phosphate formation under restricted conditions and/or by mixed, re-worked organic components that may also have had different origin (i.e., marine versus terrestrial). To investigate this issue further a wider scale study on the organic content of the sediment is necessary.

In the view of the available biostratigraphic data several interpretations can be proposed for the observed CIE in the Gafsa Basin. If the sudden occurrence of *Apectodinium* complex in the top of the section (Fig. 2a) represents the beginning of the *Apectodinium* acme then the Chouabine Fm. is much older and the CIE probably has local origin, which would also concur with the $\delta^{13}C_{org}$ data. However, this would contradict the reported NP9 nannozone for these beds (Bolle et al., 1999), though the nannofossils identified here give only uncertain NP9 age. The Tethyan *Apectodinium* acme started just before the NP9 zone (Hardenbol et al., 1998), almost at the same time when *A. homomorphum* appeared in the North Atlantic (Fig. 6). As *A. homomorphum* is common in the older beds of the Chouabine Fm. (Fig. 2a), one can correlate these beds with the NP9 zone even if this species may have appeared somewhat earlier in the Tethys. Similarly, the rare presence of *A. augustum* would also support a late Thanetian age (Williams et al., 2004). *Apectodinium* complex was already widespread in NP7/8 nannozone at the Elles section (Crouch et al., 2003), north of the Kasserine palaeo-Island (Fig. 1). Therefore, the increased amount of *Apectodinium* complex at the top of the succession could be explained by opening of the basin, which is supported by oxygen isotopic composition of shark teeth analyzed from phosphorite layer 0 (Kocsis et al., 2013).

Putting all these together two options are proposed here explaining the CIE at Kef Eddour (Fig. 6): (1) either it represents

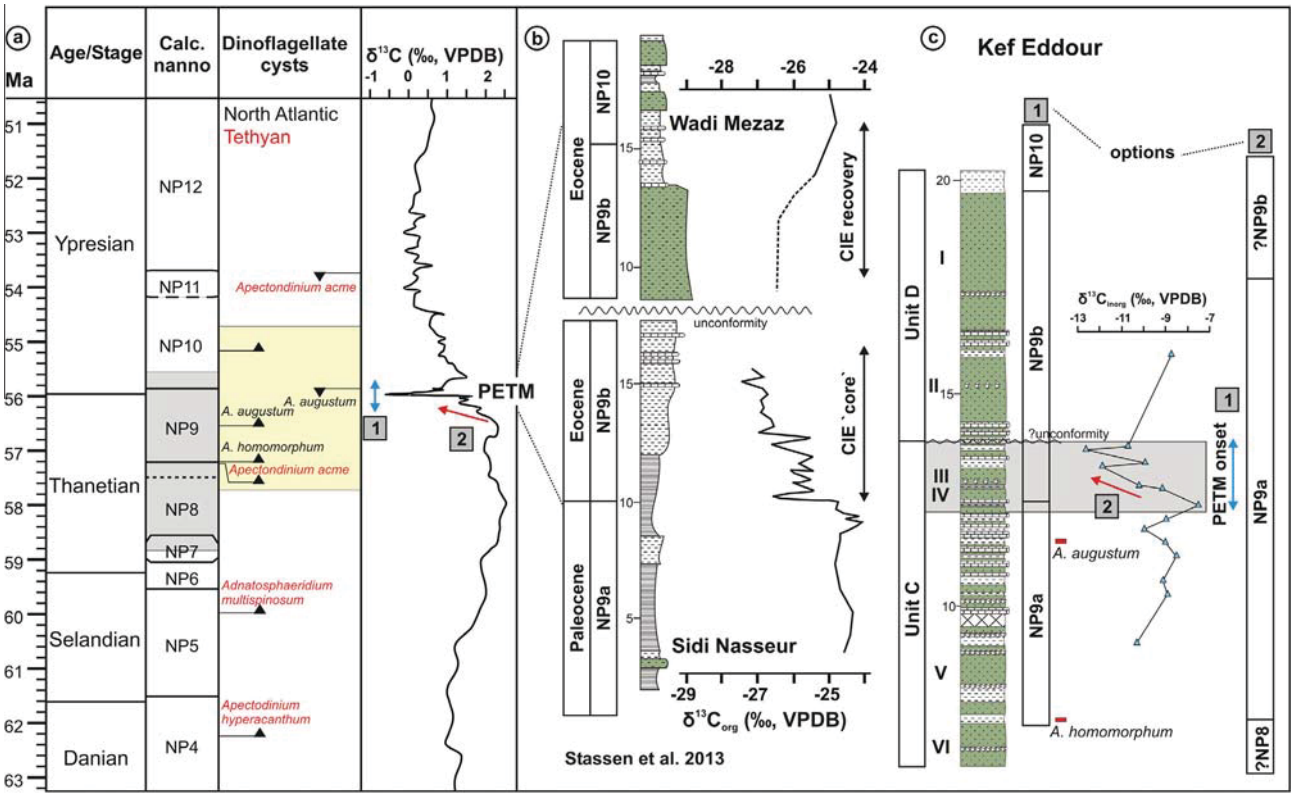

Fig. 6. (a) Calcareous nannoplankton and dinoflagellate biozonations together with the global carbon isotope curve for the early Paleogene (Hardenbol et al., 1998; Gradstein et al., 2012). The gray band covers the widest possible nannozone range for Unit C and D in the Chouabine Fm. based on Bolle et al. (1999) (see Fig. 2), while the yellow band is the same but for the dinoflagellate cysts based on Ben Abdessalam (1978) and our study (see Figs. 2 and 3). PETM – Paleocene–Eocene thermal maximum. (b) The most complete organic carbon isotopic record from Tunisia with the characteristics of the PETM event (Stassen et al., 2013). (c) The bulk inorganic carbon isotopic data from Kef Eddour. Note that the CIE (carbon isotope excursion) appears at the same level as in other part of the Gafsa Basin (cf. Fig. 2). Two possible interpretations are proposed here based on comparison with the global and the local records: (1) The Kef Eddour CIE represents the onset of the PETM event or (2) the pre-PETM isotopic record. (For interpretation of the references to colour in this figure legend, the reader is referred to the web version of this article.)

the onset of the PETM event or (2) it reflects the pre-PETM drop in the global isotope record. This isotope record is cut at the unit boundary between C and D because of a possible short gap in the sedimentation, and then the data are very sporadic due to the rather abundant phosphorite and lack of marl layers.

6. Conclusions

New geochemical (i.e., stable isotope stratigraphy) and palaeontological data provided from the Chouabine Fm. in the Gafsa Basin confirm that the major units of the phosphorite succession were deposited during the late Paleocene. Therefore, this sequence is considered as equivalent of phosphorites at the Sra Ouertane Basin (Garnit et al., 2012), but it is older than the Eocene phosphate-rich layers of Sidi Nasseur and Wadi Mezaz (Stassen et al., 2012) in northwest Tunisia. The development of the different phosphorite units can be explained by the palaeogeographic configuration and tectonic context (Chaabani, 1995; Zaïer et al., 1998).

The low diversity of benthic foraminifera and the absence of planktic forms reflect restricted conditions in the Gafsa Basin. Various diagenetic features are apparent in the sediments and developed especially on calcareous microfossils. Diagenesis is clearly dominated by processes related to phosphorite formation. Despite the diagenetic overprint, individual fossil groups have preserved offsets in $\delta^{13}C$ that may be correlated with their living environment.

Even with the obvious local effects on the palaeoenvironment, geochemical data from bulk sediments of this succession document either the onset of the global Paleocene–Eocene thermal event or the pre-PETM record.

Acknowledgements

The authors appreciate the help they received from the *Compagnie des Phosphates de Gafsa*, *Tunisia* for fieldwork in the phosphorite mining areas. We thank P. Vonlanthen for his assistance with the SEM imaging and J. Spangenberg for running samples for TOC isotopic composition. The research of L.K. was funded by the Swiss National Science Foundation (SNSF) Ambizione Grant No. PZ00P2_126407 & _145115/1. The constructive comments of two anonym reviewers are also acknowledged.

Appendix A. Supplementary material

Supplementary data associated with this article can be found, in the online version, at http://dx.doi.org/10.1016/j.jafrearsci.2014.07.024.

References

Adatte, T., Keller, G., Stinnesbeck, W., 2002. Late Cretaceous to early Paleocene climate and sea-level fluctuations: the Tunisian record. Palaeogeogr. Palaeoclimatol. Palaeoecol. 178, 165–196.

Aubry, M.P., Berggren, W.A., Stott, L., Sinha, A., 1996. The upper-Paleocene–lower Eocene stratigraphic record and the Paleocene–Eocene boundary carbon isotope excursion: implications for geochronology. In: Knox, R.W.O'.B., Corfield, R.M., Dunay, R.E. (Eds.), Correlation of the Early Paleogene in Northwest Europe. Geol. Soc. London Spec. Publ. 101, pp. 353–380.

Béji-Sassi, A., 1999. Les phosphates dans les bassins paléogènes de la partie méridionale de l'Axe Nord-Sud (Tunisie). Thèse Doct. Etat, Univ. Tunis II, Tunisie.

Belayouni, H., 1983. Etude des la matière organique dans la série phosphatée du bassin de Gafsa-Métlaoui (Tunisie): application à la compréhension des mécanismes de la phosphatogenèse. Thèse Doct. ès-Sci, Univ. Orléans, France.

Ben Abdessalam, N., 1978. Etude palynologique et micro-paléontologique de la série phosphatée du bassin de Gafsa-Métlaoui (Tunisie). Application à la compréhension des mécanismes de la phosphatogenèse. Thèse 3ème cycle, Univ. Paris VI, France.
Ben Hassen, A., Trichet, J., Disnar, J.-R., Belayouni, H., 2009. Données nouvelles sur le contenu organique des dépôts phosphatés du gisement de Ras-Draâ (Tunisie). C. R. Geosci. 341, 319–326.
Ben Hassen, A., Trichet, J., Disnar, J.-R., Belayouni, H., 2010. Pétrographie et géochimie comparées des pellets phosphatés et de leur gangue dans le gisement phosphaté de Ras-Draâ (Tunisie). Implications sur la genèse des pellets phosphatés. Swiss. J. Geosci. 103, 457–473.
Bolle, P.M., Adatte, T., Keller, G., Von Salis, K., Burns, S., 1999. The Paleocene–Eocene transition in the southern Tethys (Tunisia); climatic and environmental fluctuations. Bull. Soc. Géol. Fr. 170, 661–680.
Bornemann, A., Pirkenseer, C.M., Steurbaut, E., Speijer, R.P., 2012. Early Paleogene $\delta^{13}C$ and $\delta^{18}O$ records based on marine ostracodes: implications for the upper Danian succession at Sidi Nasseur (Tunisia) and their application value in paleoceanography. Austrian J. Earth Sci. 105, 77–87.
Burollet, P.F., 1956. Contribution à l'étude stratigraphique de la Tunisie Centrale. Ann. Mines Géol., Tunis 18, 352.
Burollet, P.F., Oudin, J.L., 1980. Paléocène en Tunisie-Pétrole et phosphate. In: Géologie comparée des gisements de phosphate et de pétrole, mémoire du BRGM, 116.
Chaabani, F., 1995. Dynamique de la partie orientale du bassin de Gafsa au Crétacé et au Paléogène: Etude minéralogique et géochimique de la série phosphatée Eocène, Tunisie méridionale. Thèse Doc. Etat, Univ. Tunis II. Tunisie.
Chaabani, F., Ben Abdelkader, O., 1992. Nouvelles données stratigraphiques sur le Paléocène du Bassin de Gafsa: Conséquence paléogéographique. Note Serv. Géol. Tunisie 59, 77–87.
Chaabani, F., Ounis, A., 2008. Sequence stratigraphy and depositional environment of phosphorite deposits evolution: case of the Gafsa basin, Tunisia. Conference abstract at the Intern. Geol. Cong. Oslo, 2008.
Crouch, E.M., Brinkhuis, H., Visscher, H., Adatte, T., Bolle, P.M., 2003. Late Paleocene–early Eocene dinoflagellate cyst records from the Tethys: further observation on the global distribution of Apectodinium. In: Wing, S.L. et al. (Eds.), Causes and Consequences of Globally Warm Climates in the Early Paleogene, Special Paper, vol. 369. Geological Society of America, pp. 113–131.
Ernst, S.R., Guasti, E., Dupuis, C., Speijer, R.P., 2006. Environmental perturbation in the southern Tethys across the Paleocene/Eocene boundary (Dababiya, Egypt): foraminiferal and clay mineral records. Mar. Micropaleontol. 60, 89–111.
Fensome, R.A., Williams, G.L., 2004. The Lentin and Williams Index of Fossil Dinoflagellates. American Association of Stratigraphic Palynologists, College Park.
Fournier, D., 1978: Nomenclature lithostratigraphique des série du Crétacé supérieur au Tertiaire de Tunisie; Bull. Cent. Rech. Explor. Prod. Elf-Aquitaine, pp. 97–1148.
Fournier, D., 1980. Phosphates et pétroles en Tunisie. In: Géologie comparée des gisements de phosphate et de pétrole. BRGM, vol. 24, pp. 157–166.
Galfati, I., Sassi, A.B., Zaier, A., Bouchardon, J.L., Bilal, E., Joron, J.L., Sassi, S., 2010. Geochemistry and mineralogy of Paleocene–Eocene Oum El Kheceb phosphorites (Gafsa-Metlaoui Basin) Tunisia. Geochem. J. 44, 189–210.
Garnit, H., Bouhlel, S., Barca, D., Chtara, C., 2012. Application of LA-ICP-MS to sedimentary phosphatic particles from Tunisian phosphorite deposits: insights from trace elements and REE into paleo-depositional environments. Chem. Erde 72, 127–139.
Gradstein, F.M., Ogg, J.G., Schmitz, M., Ogg, G., 2012. The Geological Time Scale 2012, vols. 1 & 2. Elsevier Science Ltd., Oxford, pp. 1–1176.
Hardenbol, J., Thierry, J., Farley, M.B., Jacquin, T., de Graciansky, P.-C., Vail, P.R., 1998. Mesozoic and Cenozoic sequence chronostratigraphic framework of European Basins. In: de Graciansky, P.-C., Hardenbol, J., Jacquin, T., Vail, P.R. (Eds.), Mesozoic and Cenozoic Sequence Stratigraphy of European Basins. SEPM Special Publication, vol. 60, pp. 3–14 (chart 3).
Hoefs, J., 2004. Stable Isotope Geochemistry, fifth ed. Springer, Berlin, p. 340.
Jorissen, F.J., Stigler, H.C., Widmark, J.G.V., 1995. A conceptual model explaining benthic foraminiferal microhabitats. Mar. Micropaleontol. 26, 3–15.
Kennett, J.P., Stott, L.D., 1991. Abrupt deep-sea warming, palaeoceanographic changes and benthic extinctions at the end of the Palaeocene. Nature 353, 225–229.
Koch, P.L., Zachos, J.C., Gingerich, P.D., 1992. Correlation between isotope records in marine and continental carbon reservoirs near the Palaeocene/Eocene boundary. Nature 358, 319–322.
Kocsis, L., Ounis, A., Chaabani, F., Salah, M.N., 2013. Paleoenvironmental conditions and strontium isotope stratigraphy in the Paleogene Gafsa Basin (Tunisia) deduced from geochemical analyses of phosphatic fossils. Int. J. Earth Sci. (Geol. Rundsch) 102, 1111–1129.
Kocsis, L., Gheerbrant, E., Mouflih, M., Cappetta, H., Yans, J., Amaghzaz, M., 2014. Comprehensive stable isotope investigation of marine biogenic apatite from the late Cretaceous–early Eocene phosphate series of Morocco. Palaeogeogr. Palaeoclimatol. Palaeoecol. 394, 74–88.
Kolodny, Y., Luz, B., 1992. Isotope signatures in phosphate deposits: formation and diagenetic history. In: Clauer, N., Chaudhuri, S. (Eds.), Isotopic Signatures and Sedimentary Records. Lect. Notes Earth Sci., vol. 43, pp. 69–121.
Kouwenhoven, T.J., Speijer, R.P., van Oosterhout, C.W.M., van der Zwaan, G.J., 1997. Benthic foraminiferal assemblages between two major extinction events: the Paleocene El Kef section, Tunisia. Mar. Micropaleontol. 29, 105–112.
Lamboy, M., 1993. Phosphatization of calcium carbonate in phosphorites: microstructure and importance. Sedimentology 40, 53–62.
Lawrence, J.R., 1989. The stable isotope geochemistry of deep-sea pore water. Handbook of Environmental Isotope Geochemistry, vol. 3. Elsevier, New York, pp. 317–356.
Lerman, A., Clauer, N., 2007. Stable isotopes in the sedimentary record. In: Treatise on Geochemistry, vol. 7, No. 16, pp. 1–55.
Lourens, L.J., Sluijs, A., Kroon, D., Zachos, J.C., Thomas, E., Röhl, U., Bowles, J., Raffi, I., 2005. Astronomical pacing of late Palaeocene to early Eocene global warming events. Nature 435, 1083–1087.
Lucas, J., Prévôt-Lucas, L., 1996. Tethyan phosphates and bioproductites. In: Nairn, A.E. et al. (Eds.), The Ocean Basins and Margins, vol. 8. Plenum Press, The Tethys Ocean, pp. 367–391.
Martin, W.R., Sayles, F.L., 2003. The recycling of biogenic material at the seafloor (7.02). In: Treatise on Geochemistry, vol. 7, No. 02, pp. 37–65.
McArthur, J.M., Benmore, R.A., Bremner, J.M., 1980. Carbon and oxygen isotopic composition of structural carbonate in sedimentary francolite. J. Geol. Soc. (Lond.) 137, 669–673.
McArthur, J.M., Benmore, R.A., Coleman, M.L., Soldi, C., Yeh, H.W., O'Brien, G.W., 1986. Stable isotopes characterisation of francolite formation. Earth Planet. Sci. Lett. 77, 20–34.
Morsi, A.M., Speijer, R.P., Stassen, P., Steurbaut, E., 2011. Shallow marine ostracode turnover in response to environmental change during the Paleocene–Eocene thermal maximum in northwest Tunisia. J. Afr. Earth Sci. 59, 243–268.
Nathan, Y., 1984. The mineralogy and geochemistry of phosphorites. In: Nriagu, J.O. et al. (Eds.), Photosphate Minerals. Springer-Verlag, Berlin, Heidelberg, pp. 275–290 (Chapter 8).
Ounis, A., Kocsis, L., Chaabani, F., Pfeifer, H.-R., 2008. Rare earth element and stable isotope geochemistry ($\delta^{13}C$ and $\delta^{18}O$) of phosphorite deposits in the Gafsa Basin, Tunisia. Palaeogeogr. Palaeoclimatol. Palaeoecol. 268, 1–18.
Ounis, A., 2011. Apport de la géochimie des Terres Rares et des isotopes pour la compréhension des mécanismes de la phosphatogenèse: exemple de la partie occidentale du bassin de Gafsa-Métlaoui. PhD Thesis, University El Manar, Tunis, p. 198.
Pagani, M., Pedentchouk, N., Huber, M., Sluijs, A., Schouten, S., Brinkhuis, H., Sinninghe Damste, J.S., Dickens, G.R., the Expedition 302 Scientists, 2006. Arctic hydrology during global warming at the Palaeocene/Eocene thermal maximum, vol. 442, pp. 671–675.
Pervinquière, L., 1903. Etude géologique de la Tunisie central. In: De Rudeval, F.R. (Ed.), Paris, p. 360.
Piper, D.Z., Kolodny, Y., 1987. The stable isotopic composition of a phosphate deposit: $\delta^{13}C$, $\delta^{34}S$ and $\delta^{18}O$. Deep-Sea Res. 34, 897–911.
Prévôt, L., 1990. Geochemistry, Petrography, Genesis of Cretaceous-Eocene Phosphorites: Memoirs of the Geological Society of France, vol. 158, pp. 1–232.
Sassi, S., Jacob, C., 1972. Découverte de clinoptilolite dans le bassin de Métlaoui (Tunisie). C. R. Acad. Sci. Paris 274, 1128–1131.
Sassi, S., 1974. La sédimentation phosphatée au Paléocène dans le Sud et le Centre Ouest de la Tunisie. Thèse Doct. ès-Sci, Univ. Paris-Sud Orsay, France.
Shemesh, A., Kolodny, Y., Luz, B., 1988. Isotope geochemistry of oxygen and carbon in phosphate and carbonate of phosphorite francolite. Geochimi. Cosmochim. Acta 52, 2565–2572.
Sluijs, A., Brinkhuis, H., Schouten, S., Bohaty, S.M., John, C.M., Zachos, J.C., Sinninghe Damsté, J.S., Crouch, E.M., Dickens, G.R., 2007. Environmental precursors to light carbon input at the Paleocene/Eocene boundary. Nature 450, 1218–1221.
Spoetl, C., Vennemann, T.W., 2003. Continuous-flow IRMS analysis of carbonate minerals. Rapid Commun. Mass Spectrom. 17, 1004–1006.
Stassen, P., Dupuis, C., Morsi, A.M., Steurbaut, Speijer, R.P., 2009. Reconstruction of a latest Paleocene shallow-marine eutrophic paleoenvironment at Sidi Nasseur (Central Tunesia) based on foraminifera, ostracoda, calcareous nannofossils and stable isotopes ($\delta^{13}C$, $\delta^{18}O$). Geol. Acta 7, 93–112.
Stassen, P., Dupuis, C., Steurbaut, E., Yans, J., Speijer, R.P., 2012. Perturbation of a Tethyan coastal environment during the Paleocene–Eocene thermal maximum in Tunisia (Sidi Nasseur and Wadi Mezaz). Palaeogeogr. Palaeoclimatol. Palaeoecol. 317–318, 66–92.
Stassen, P., Dupuis, C., Steurbaut, E., Yans, J., Storme, J.-Y., Morsi, A.-M., Iacumin, P., Speijer, R.P., 2013. Unraveling the Paleocene–Eocene thermal maximum in shallow marine Tethyan environments: the Tunisian stratigraphic record. Newsl. Stratigr. 46 (1), 69–91.
Thomas, P., 1885. Sur la découverte de gisements de phosphate du chaux dans le sud de la Tunisie. C. R. l'Académie Sci., Paris 101, 1184.
Thomas, D., Zachos, J., Bralower, T., Thomas, E., Bohaty, S., 2002. Warming the fuel for the fire: evidence for the thermal dissociation of methane hydrate during the Paleocene–Eocene thermal maximum. Geology 30, 1067–1070.
Van der Zwaan, G.J., Duijnstee, I.A.P., den Dulk, M., Ernst, S.R., Jannink, N.T., Kouwenhoven, T.J., 1999. Benthic foraminifers: proxies or problems? A review of paleocological concepts. Earth Sci. Rev. 46, 213–236.
Visse, L., 1952. Genèse des gîtes phosphatés du sud-est Algéro-Tunisien. 19ème congrés géologique Inter., Algerie, pp. 1–58.
Williams, G.L., Brinkhuis, H., Pearce, M.A., Fensome, R.A., Weegink, J.W., 2004. Southern Ocean and global dinoflagellate cyst events compared: index events for the Late Cretaceous–Neogene. In: Exon, N.F., Kennett, J.P., Malone, M.J. (Eds.), Proc. ODP, Sci. Results, vol. 189, pp. 1–98.
Wefer, G., Berger, W.H., 1991. Isotope paleontology: growth and composition of extant calcareous species. Mar. Geol. 100, 207–248.
Wood, G.D., Gabriel, A.M., Lawson, J.C., 1996. Palynological techniques – processing and microscopy. In: Jansonius, J., McGregor, D.C. (Eds.), Palynology: Principles and Applications: American Association of Stratigraphic Palynologists Foundation, pp. 29–50.

Yans, J., Amaghzaz, M., Bouya, B., Cappetta, H., Iacumin, P., Kocsis, L., Mouflih, M., Selloum, O., Sen, S., Storme, J.-Y., Gheerbrant, E., 2014. First carbon isotope chemostratigraphy of the Ouled Abdoun phosphate Basin, Morocco; implications for dating and evolution of earliest African placental mammals. Gondwana Res. 25, 257–269.
Zachos, J., Pagani, M., Sloan, L., Thomas, E., Billups, K., 2001. Trends, rhythms, and aberrations in global climate 65 Ma to present. Science 292, 686–693.
Zachos, J.C., Dickens, G.R., Zeebe, R.E., 2008. An early Cenozoic perspective on greenhouse warming and carbon-cycle dynamics. Nature 451, 279–283.
Zazzo, A., Lécuyer, C., Mariotti, A., 2004. Experimentally-controlled carbon and oxygen isotope exchange between bioapatites and water under inorganic and microbially mediated conditions. Geochim. Cosmochim. Acta 68, 1–12.
Zaïer, A., Beji-Sassi, A., Sassi, S., Moody, R.T.J., 1998. Basin evolution and deposition during the Early Paleocene in Tunisia. In: Macgregor, D.S., Moody, R.T.J., Clark-Lowes, D.D. (Eds.), Petroleum Geology of North Africa. Geol. Soc. London Spec. Publ., vol. 132, pp. 375–393.